Vortex Fluidic Chemical Transformations

Dr. Joshua Britton[a,b], **Dr. Keith A. Stubbs**[c], **Prof. Dr. Gregory A. Weiss**[a], and **Prof. Dr. Colin L. Raston**[b]

[a]Department of Chemistry, University of California, Irvine, CA, USA 92697-2025

[b]Centre for NanoScale Science and Technology, School of Chemical and Physical Sciences, Flinders University, Adelaide, SA, Australia 5001
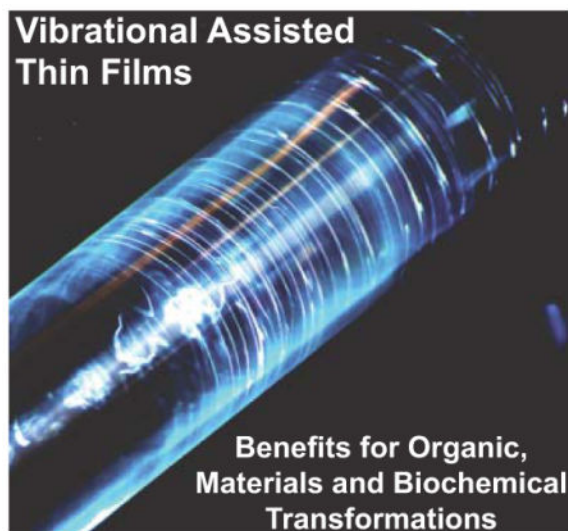
[c]School of Molecular Sciences, The University of Western Australia, Crawley, WA, Australia

Abstract

Driving chemical transformations in dynamic thin films represents a rapidly thriving and diversifying research area. Dynamic thin films provide a number of benefits including large surface areas, high shearing rates, rapid heat and mass transfer, micromixing, and fluidic pressure waves. Combinations of these effects provide an avant-garde style of conducting chemical reactions with surprising and unusual outcomes. The vortex fluidic device (VFD) has proved its capabilities in accelerating and increasing the efficiencies of numerous organic, materials and biochemical reactions. This MiniReview surveys transformations that have benefited from VFD-mediated processing, and identifies concepts driving the effectiveness of vortex-based dynamic thin films.

Graphical Abstract

Many organic, materials and biochemical transformations benefit from vibrational responses within thin films. Over the last few years an international collaboration has explored these effects on several scientific disciplines. This MiniReview encapsulates these outcomes and critically examines how vortexing thin films drives creative approaches to chemical processes.

Correspondence to: Gregory A. Weiss; Colin L. Raston.

Vibrational Assisted Thin Films

Benefits for Organic, Materials and Biochemical Transformations

Keywords

Thin films; Continuous Flow; Vortex Fluidics; Biochemistry; Organic synthesis

1. Introduction

Performing chemical reactions within the confines of dynamic thin films can offer a range of benefits over conventional processing in a round bottom flask. Within dynamic thin films, high heat and mass transfer, shear stress and micromixing[1] can lead to the improved syntheses of polymers,[2] chemicals[1c, 3] and materials.[4]

Dynamic thin films are generated by the continuous addition of fluid to a rapidly rotating surface. Once the fluid has been injected, centrifugal forces drive formation of a thin film that stretches across the surface of the reactor (Video 1, 2 and Figure 1D). Seminal research in this area focused around the spinning disk reactor (SDR)[1a] and rotating tube processor (RTP) to generate dynamic thin films for academic and industrial chemical processes. [1c, 2a, 3–4, 4c, 5] Although beneficial, this discipline remained mostly localized to process intensification; it is possible that the large volumes of sample required (>50 mL) and high capital costs deterred researchers from exploring this area. In addressing this, a vortex fluidic device (VFD) was designed to subject both small sample sizes (1 mL or less) and continuous flow operations to the benefits of dynamic thin films. The VFD has now emerged as a cost effective research tool.

Much like the SDR and RTP, the VFD mediates reactions in dynamic thin films that result from the rapid rotation (2–10 krpm) of an *angled* sample tube (Figure 1, Video 3). The VFD operates in either a *confined,* or a *continuous flow* operation. The confined mode of operation rotates a sample tube (optionally sealed) holding a finite volume of liquid. In the continuous flow mode, reagents are continually introduced into the rotating sample tube *via* jet feeds. As fluid enters the system, the droplet impacts the hemisphere of the rotating tube to form a thin film (35 – 76 μm thick, Figure 1D).[6] The initial interplay between the fluid

and the reactor surface generates high levels of micromixing and shear stress (14 – 31 Pa for n-butanol)[6]. After formation of the thin film, the fluid proceeds up the inner surface of the reactor as more fluid is added, with the resulting film 200 μm thick.[9] While the fluid climbs the inner surface of the reactor, reagents are continually exposed to shear stress from the Stewartson/Ekman layers and native vibrational affects. These physical properties can provide a unique environment for controlling chemical reactivity (Video 3, Figure 1A).

The last four years of experimentation has demonstrated that the VFD has several benefits over the SDR and RTP. These include: (*i*) increased residence times for continuous flow applications, (*ii)* a confined mode of operation for exploring small sample volumes for biochemical and materials applications, and (*iii*) vibrations native to the VFD can drive unusual reaction outcomes.

Although vibrational effects in reactions have been documented, the vibrations present in the VFD are distinctly different. The VFD functions through the rapid rotation of a glass sample tube. At these very high rotational speeds, potentially, even the slightest misalignment or bearing unevenness could introduce vibrations in the system. When the sample tube experiences such vibrations, it is termed a primary mechanical response. As there is fluid on the inner surface of the sample tube during rotation, a secondary fluid dynamical response is imparted into the fluid creating dynamic pressure waves in the thin film (Figure 1C).[6, 7b, 8] Importantly, removing the bearings holding the sample tube and other major sources of vibration in the system eliminates the generation of beneficial Faraday waves. Furthermore, vibrational contributions to transformations occur at specific rotational speeds, not over a broad range as predicted for a non-mechanical effect. These vibrations are now well documented, and have been the focus of several research projects.[6, 7b, 9] In exploring the benefits of VFD conditions on chemical reactions, we here review VFD-mediated acceleration of (*i*) synthetic, (*ii*) materials and (*iii*) biochemical transformations.

2. Organic Transformations

Accelerating the Diels-Alder reaction of cyclopentadiene through VFD processing provided a model system to explore the large number of VFD-operating parameters (Figure 2A).[10] The sample tube inclination angle and rotational speed were the most important variables identified. The tilt angle of the sample tube is crucial for the generation of vibrations in the thin film. Control experiments demonstrated that a 45° tilt angle provided the necessary vibrations to accelerate chemical transformations. Changing the tilt angle of the reactor, or removing device-specific variations eliminates VFD-mediated enhancement. Furthermore, although a 90° tilt angle was optimal for rate acceleration, a 45° tilt angle, shown to be second best, was chosen for continuous flow operation. Rotational speed is always the most crucial variable in all reported transformations, and for this specific Diels-Alder reaction, rotational speeds of >2 krpm resulted in an increase in yield compared to the non-VFD control. This increase seemed directly proportional to the rotational speed; however, a 3 krpm rotational speed generated unusually higher levels of conversion. Initially this was reasoned to be due to variable levels of shear stress, a hypothesis repeated in some initial papers.[10–11] However, higher rotational speeds, which can be expected to increase shear stress, often decreases reaction yields.[6, 7b, 9a, 12] Thus, shear stress is unlikely to solely

drive the observed increase in reaction yields and rates. Continued investigation has generated fundamental understanding of the unique attributes of reactions processed in a VFD. First, transformations performed in the VFD are often reliant on specific rotational speeds to induce beneficial vibrations for enhanced chemical yields. Second, the tilt angle of the device is crucial; deviation away from optimal angles can decrease chemical yields. Lastly, the diameter of the sample tube can affect the reaction outcome. Taking into account these observations, optimization of new reactions requires systematic exploration of these variables; the bottleneck for enhanced chemical yield often lies in variation of the rotational speed.

Next, more demanding Diels-Alder reactions between anthracene derivatives and *N*-phenylmaleimide that only yielded 15% conversion in a round bottom flask after five hours were studied.[13] These transformations typically require long reaction times, heat,[14] and bases for good conversion.[15] Conducting reactions under identical conditions in the VFD at a 5 krpm rotational speed generated quantitative yields (Figure 2A). Again, the rotational speed of the sample tube defined the ability of the VFD to obtain high levels of conversion. Variation of 1 krpm either side of the optimum rotational speed decreased reaction yields by ≈10–15%. Notably, a ≈5 krpm rotational speed has generated optimal conversion for VFD transformations in other unrelated materials, organic, and biochemical systems.[7a, 16] This observation suggests a resonance effect inherent to the VFD due to the strict criteria for a specific rotational speed. If there was a linear effect of the rotational speed on yield, it could be related to shear stress, however, the sharpness of the response in this rapidly rotating system is indicative of a mechanical response. To highlight this point further, eliminating major vibrations in the system (through removal of the bearings) removed the conditions required for enhanced yields.[7b]

Dynamic thin films have inherently good mass and heat transfer, whereas reactions in round bottom flasks have relatively poor mixing and heat transfer (especially at larger scales). These properties are often the lead cause for difficulties in reaction scale-up.[17] Processing in thin films can overcome these issues as demonstrated with the synthesis of 2,4,6-triarylpyridines (Figure 2B).[18],[10] Here, VFD-mediated conditions favored Michael addition over Schiff-base formation. This chemoselectivity contrasts the outcome in a round bottom flask, where uneven heating prevails and the opposite result occurs.[19]

Tuned VFD-mediated reactions can also generate kinetic over thermodynamic products. Kinetic control was possible in the synthesis of macrocyclic resorcin[4]arenes and pyrogallo[4]arenes (Figure 2C).[20] Condensation using both the VFD, and non-VFD conditions produced the thermodynamically favored isomers, with the exception of the condensation of vanillin and pyrogallol. In the latter reaction, the thermodynamic and kinetic isomers were produced in a 3:4 ratio respectively. Through further optimization of VFD conditions, a 7:3 ratio of kinetic: thermodynamic isomers was obtained in a 96% yield (>95% purity by 1H NMR, Figure 2C). In contrast to VFD processing (*minutes required*), converting a thermodynamic isomer into a kinetic isomer typically *requires five days* at reflux.

Increased reaction yields and rates often result from VFD processing. Carbon-nitrogen bond formation *via* S_NAr mechanism is sluggish without a transition metal catalyst. VFD processing increased the rate of this reaction, allowing the reaction to be conducted without addition of a transition metal catalyst.[11b] Coupling 2-chloropyrazine with a range of amines generated analogues in high yield in the confined mode (12 h reaction times). Obviating the need for expensive and waste-producing catalysts by accelerating reactions could allow the development of more sustainable reaction chemistry.

While many reactions in this Review benefit from micromixing, mass transfer, and vibrational effects, photoredox reactions benefit from the large surface area of the thin film. The Beer-Lambert law highlights the need for efficient light penetration to drive efficient photoredox transformations in solution. The high surface area provides optimal conditions for photoredox acceleration; uniform coverage of green LED lights around the sample tube generated yields up to 95%. Optimal conditions for continuous flow required a 4 krpm rotational speed with a 50 μL min^{-1} flow rate. Again, this transformation achieved good yields at a multitude of rotational speeds, but, a rotational speed optimization found the necessary vibration at 4 krpm to generate greater yields.[11a]

As continuous flow chemistry continues to thrive, the ability of the VFD to facilitate this area has been explored. Amides,[21] biodiesel,[12, 16] esters,[7b] tri-alkylpyridines[10, 18] and photoredox products[11a] have benefited from VFD-based continuous flow. The high heat transfer present in the VFD has been used to improve the yields of acylation reactions using acyl chlorides. These exothermic reactions, if not controlled, lead to reagent degradation and safety concerns. Processing in a VFD with high heat transfer avoids such concerns while providing improved yields for the formation of 27 amides including the synthesis of ureas, modified amino acids and pre-drug motifs (70 second residence time, Figure 2E). The short residence times of these reactions lead to the discovery of a rapid deprotection of benzylated amines at room temperature; this deprotection reaction usually requires a catalyst and heating. The interchangeable nature of reagents in continuous flow by exchanging feed inlets allows rapid testing of many substrates and reaction conditions.

Continuous flow in the VFD enables multi-step reactions. First, the fluid outlet from one VFD can be fed into a second VFD and so on. Each VFD mediates a different transformation to increase the level of molecular complexity as non-isolated synthetic intermediates pass from one device to another. This concept was first demonstrated in the VFD with the synthesis of the local anesthetic, lidocaine.[21] Here, the amide is synthesized in the first VFD before the solution is passed into a second VFD for *in situ* solvent exchange and S_N2 substitution. The total residence time for the synthesis of lidocaine was only nine minutes, generating 153 mg h^{-1} (>95% purity observed by ^{1}H NMR analysis) of this active pharmaceutical ingredient (API). *In situ* solvent exchange in a continuous flow reactor is a useful technique, especially at standard temperature and pressure. For example, water evaporation occurs roughly ten-fold faster compared to non-VFD conditions. Separately, such dehydration can increase rates for the synthesis of esters[6, 7b] and imines during condensation reactions.[8] Secondly, drawing inspiration from Nature's method for building up molecular complexity, an assembly line style synthesis applies multiple synthetic transformations along the length of a single sample tube. For the synthesis of lidocaine, the

amine and acyl chloride were injected into the hemisphere of the sample tube, and acylation occurred over the first 5 cm. Next, *in situ* solvent exchange for DMF and S_N2 substitution occurs with diethylamine at 60 °C over the final 9.5 cm of the tube. This style of sequential processing produced 27 mg h^{-1} of lidocaine after isolation through silica chromatography and recrystallization (Figure 2D). Furthermore, this style of control in reactivity has also been used to rapidly synthesize an α-aminophosphonate in high yield (80%, >99% purity with crystals suitable for X-ray analysis) in only a seven minute residence time with the use of column chromatography for isolation of the single product (Figure 2D).[8]

3. Materials Transformations

The first materials transformation driven by the VFD was the disassembly of molecular capsules in developing versatile drug delivery systems. Two *p*-phosphonic acid calix[5]arene molecules held together by a seam of H-bonds disassemble under shear stress, with the capsule then binding carboplatin in building a capsule for chemotherapy medicine (Figure 3A).[22] More recently, ≈100 nm diameter self assembled vehicles based on *O*-alkyl calix[4]arenes as phospholipid mimics has been developed for drug delivery, with the uptake of carboplatin in the vehicles increasing from undetectable levels in a round bottom flask to 75% with VFD processing. These high-loaded vehicles have a 4.5-fold increase in carboplatin loading efficiency on ovarian cancer cells relative to non-vehicle delivered carboplatin. A control reaction with sonication provided only 17% uptake of carboplatin in the vehicles, further providing evidence for vibrational driven uptake.[11e] Just as VFD-mediated organic transformations are affected by Faraday waves, they also appear to be important in materials transformations. This section critically examines contributions by vibrations, mass transfer, and shear stress on materials processing using a VFD thin film microfluidic platform.

Graphene has unique properties for a range of applications in materials and condensed-matter physics.[23] Methods developed for the generation of graphene include probe sonication and chemical vapor deposition. However, these processes are energy intensive, and can result in both chemical degradation and the introduction of defects. Graphite and its iso-electronic and iso-structural analogue, hexagonal boron nitride (*h*-BN) can be exfoliated into individual sheets within the VFD with little or no degradation (Figure 3B). Exfoliation is rotational speed dependent, with graphene and *h*-BN requiring 7 krpm and 8 krpm rotational speed respectively.[11d] At rotational speeds 1 krpm away from this optimal speed, little exfoliation occurs. This observation suggests this process is unlikely to rely solely on shear stress and a vibrational response analogous to sonication could drive exfoliation in the VFD.

VFD-processing can also drive the bending of single walled carbon nanotubes (SWCNT) to form tightly packed toroids and other ring-like structures (Figure 3F).[11c] This transformation critically requires a 1:1 solvent mixture of water and toluene. As hypothesized, the interfacial tension between the two liquids could facilitate bending of the SWCNTs. Variation of the sample tube diameter generated different diameter toroids, demonstrating a dependency on the fluid dynamics of the system. A 10 mm external diameter sample tube produced 100 to 200 nm diameter toroids, whilst a 20 mm external

diameter sample tube produced 300 to 700 nm diameter toroids. Not surprisingly, only at a 7.5 krpm rotational speed this process is effective; further supporting the hypothesis that vibrational contributions in the thin film are paramount for this unique VFD-mediated processing. Interestingly, longer reaction times (one hour) resulted in the formation of 'figure eight structures'. A non-VFD process control reaction using probe sonication also generated such structures, and given probe sonication uses intense vibrations, these results are consistent with the VFD-mediated transformation being vibrational induced. Irradiating colloidal suspensions of SWCNTs in a 1:1 mixture of water and NMP with a pulsed laser operating at 1064 nm, results in slicing of CNTs, and similarly the slicing of DWCNTs and MWCNTs (Figure 3E).[9b] Slicing occurs at a 7.5 krpm rotational speed, with 7.55 and 7.45 krpm being ineffective. The specificity for this rotational speed strongly supports VFD-mediated transformation that are not solely reliant on shear stress, with the bending likely to be vibrational induced, and the high energy laser source rupturing the strained bonds, mediating slicing of the CNTs.

Controlling polymorphs of crystals or minerals is important for both fundamental understanding and applications such as in pharmaceutical synthesis. Calcium carbonate polymorphs can be controlled through VFD-mediated processing.[24] The intense micromixing of the VFD transforms vaterite into calcite, the thermodynamically more stable polymorph. Under non-VFD-mediated conditions (refluxing in ethanol at 80 °C), the calcite polymorph was converted into aragonite (64%) and vaterite (34%) polymorphs. Processing at 4.5 krpm under the same conditions provided quantitative conversion to calcite. Rotational speeds at either side of the optimal gave similar results as the non-VFD-mediated control, which again provides strong evidence for vibration-driven transformations. As previously shown, sonication can control formation of specific polymorphs, and the intensity of the vibrations can determine the materials' properties. Thus, subtle and controlled vibrations in these thin films can provide similar effects (Figure 3E).[24b, 25]

Recently, uniform tubules of face-centred cubic *(fcc)* fullerene C_{60} *ca.* 0.4 to 3 μm in length with hollow diameters 100 to 400 nm were created.[26] This was achieved by subjecting a 1:1 mixture of toluene and water in the absence of surfactants at a 7 krpm rotational speed at a 45° tilt angle. Operating at other rotational speeds and inclination angles resulting in a mixture of nanostructures with no control over morphology. This example further highlights the ability of a vibrational induced Faraday wave to control materials processes, with the non-VFD control requiring surfactants and downstream processing to generate the solvent free *fcc* phase.

Fabricating mesoporous silica and silica xerogels under VFD continuous flow conditions allowed control over the physical and chemical properties of the material.[27] In the VFD, gram-scale quantities of SBA-15 mesoporous silica were synthesized under ambient conditions with a significantly reduced pre-calcination time (Figure 3C). As with the formation of SWCNT toroids and slicing of CNT's (*vide supra*), varying rotational speeds can control the material's physical properties. At higher rotational speeds, the thin film drives intense micromixing of otherwise immiscible liquids, as well as evaporation of the ethanolic byproduct during the condensation reaction, accelerating formation of mesoporous silica and the gelation time of silica xerogels. Controlling ethanol removal can also control

the pore size, as previously shown.[28] In conclusion, hydrothermal treatment for long time periods (≈48 h) can be avoided with this VFD-mediated process.

4. Biochemical Transformations

As demonstrated for other chemical processes, biochemical transformations can also be accelerated and controlled in the VFD. Biocatalysis, drug delivery and protein refolding have elucidated mechanical aspects and fundamental knowledge about protein reactivity and conformation, whilst providing practical solutions. Pharmaceutical, industrial and agricultural applications rely heavily upon laborious conventional methods for protein refolding. A VFD-mediated approach refolded four proteins including hen egg white lysozyme (HEWL) and cAMP-dependant protein kinase A (PKA, Figure 4A).[7a] Refolding times were reduced by a factor of 100 and impressively, refolding a larger, more complex protein, caveolin-1, resulted in a 10^3 reduction in refolding time. Protein refolding benefits from the shear stress in the fluid to isolate folding intermediates while preventing tangling. Furthermore, vibrations created at specific rotational speeds are hypothesized to drive hydrophobic collapse *via* pressure effects associated with Faraday waves. For example, the optimal rotational speed for refolding HEWL was 5.00 krpm, variation away from this rotational speed decreased levels of folded protein (Figure 4B).

Since VFD-induced Faraday waves promote protein folding, we reasoned that the vibrations native to the VFD could accelerate biocatalysis. As enzymes spatially rearrange during a catalytic event (for closing and opening motions), Faraday waves could drive such motions with changes in pressure. When VFD-Faraday waves were applied to four enzymes and their substrates (esterase, alkaline phosphatase, β-glucosidase and deoxyribose-phosphate aldolase (DERA)), enzymatic activity was accelerated in all cases relative to a control reaction in an Eppendorf tube.[9a] DERA, for example, achieved a maximum of 26-fold acceleration by VFD processing occurred relative to the non-processed reaction. We believe that the acceleration effect is more pronounced for DERA due to the relatively low catalytic rate of this enzyme; esterase and lipase on the other hand are relatively rapid. As all proteins tested had requirements for specific rotational speed, this most likely reflects differences in the structure and properties of each enzyme (Figure 4C). Furthermore, either side of the optimal rotational speed decreased catalytic acceleration. This approach could allow a large range of enzymes to be accelerated at standard temperature and pressure with little optimization, and importantly, no genetic modification. Currently, high-pressure reactors can drive enzymatic transformations,[31] it is thus conceivable to believe that a room temperature and pressure approach could be beneficial.

Finally, bioconjugation and spatial segregation of enzymes onto the surface of the sample tube has been achieved (Figure 4D).[30, 32] Using fused His_n-tags proteins for bioconjugation with immobilized metal affinity chromatography (IMAC) resin allowed ten-minute purification and creation of a "reactor ready" system in a single continuous flow process. This proof of concept allowed six different proteins to be purified from complex cell lysate, including tobacco epi-aristolochene synthase (TEAS), a difficult, yet valuable biocatalyst. While rapid purification and bioconjugation affords a simple approach to continuous flow

multi-step biocatalysis, spatial segregation into ordered zones opens up possibilities for controlling multi-step enzymatic pathways in organic synthesis.

5. Summary and Outlook

In conclusion, the VFD has impacted several fields in a relatively short timeframe. Each result from disparate experimental systems provides strong and previously unappreciated evidence for vibration-based transformations. These results suggest that VFD-mediated transformations have only begun to impact diverse processes and applications. We expect that the VFD could accelerate a wide range of transformations through subjecting samples to pressure waves. The acceleration in reactivity along, with access to otherwise difficult to achieve products provides a strong basis for continued evolution of the technique for greener, less laborious scientific and industrial techniques and applications.

Major research efforts are required for further advancing VFD technology, including a detailed understanding of the complex fluid dynamics at play which vary along the tube. This could be aided by theoretical studies, which includes predicting rotational speeds required for specific synthetic, materials, and biochemical transformations, for rapid streamlining reaction optimization. In addition, automation/robotic control of VFD processing could further aid the optimization of processing, for both confined and continuous flow modes of operation. Overall, for VFD processing to become popular, automation/robotic control is important for fast tracking the exploration and the dissection of the thin film microfluidic platform's influence on chemical reactivity and selectivity. Thus far, a number of proteins have been folded and accelerated, and a number of organic transformations and materials fabrications (bottom up and top down) have been explored. Finally, the availability of VFD technology needs to be addressed which could include 3D printing of key components.

Supplementary Material

Refer to Web version on PubMed Central for supplementary material.

Acknowledgments

References

1. a) Boodhoo KVK, Jachuck RJ. Appl Therm Eng. 2000; 20:1127–1146.b) Meeuwse M, van der Schaaf J, Kuster BFM, Schouten JC. Chem Eng Sci. 2010; 65:466–471.c) Chen X, Smith NM, Iyer KS, Raston CL. Chem Soc Rev. 2014; 43:1387–1399. [PubMed: 24346239]

2. a) Pask SD, Nuyken O, Cai Z. Polymer Chem-UK. 2012; 3:2698–2707.b) Dobie CG, Vicevic Marija, Boodhoo KVK. Chem Eng Process: Process Intensification. 2013; 71:97–106.

3. Oxley P, Brechtelsbauer C, Ricard F, Lewis N, Ramshaw C. Ind Eng Chem Res. 2000; 39:2175–2182.

4. a) Mohammadi S, Harvey A, Boodhoo KVK. Chem Eng J. 2014; 258:171–184.b) Liu HS, Wang YH, Li CC, Tai CY. Chem Eng J. 2012; 183:466–472.c) Tai CY, Wang YH, Liu HS. AIChE Journal.

2008; 54:445–452.d) Tai CY, Wang YH, Tai CT, Liu HS. Ind Eng Chem Res. 2009; 48:10104–10109.

5. a) Cowen, G., Norton-Berry, P., Steel, ML. US. 4,311,570. 1982. b) Chen K-J, Chen Y-S. Chem Eng Process: Process Intensification. 2014; 78:67–72.c) Pask SD, Cai Z, Mack H, Marc L, Nuyken O. Macromol React Eng. 2013; 7:98–106.d) Feng X, Patterson DA, Balaban M, Fauconnier G, Emanuelsson EAC. Chem Eng J. 2013; 221:407–417.e) Dabir H, Davarpanah M, Ahmadpour A. Appl Physics A. 2015; 120:105–113.f) Cheong SI, Choi KY. J Appl Polymer Sci. 1995; 58:1473–1483.g) Cafiero LM, Baffi G, Chianese A, Jachuck RJJ. Ind Eng Chem Res. 2002; 41:5240–5246.

6. Britton J, Dalziel SB, Raston CL. Green Chem. 2016; 18:2193–2200.

7. a) Yuan TZ, Ormonde CFG, Kudlacek ST, Kunche S, Smith JN, Brown WA, Pugliese KM, Olsen TJ, Iftikhar M, Raston CL, Weiss GA. ChemBioChem. 2015; 16:393–396. [PubMed: 25620679] b) Britton J, Dalziel SB, Raston CL. RSC Adv. 2015; 5:1655–1660.

8. Britton J, Castle JW, Weiss GA, Raston C. Chem Eur J. 2016; 22:10773–10776. [PubMed: 27198926]

9. a) Britton J, Meneghini LM, Raston CL, Weiss GA. Angew Chem Int Ed. 2016; 55:11387–11391.Angew Chem. 2016; 128:11559–11563.b) Vimalanathan K, Gascooke JR, Suarez-Martinez I, Marks NA, Kumari H, Garvey CJ, Atwood JL, Lawrance WD, Raston CL. Sci Rep. 2016; 6:22865. [PubMed: 26965728]

10. Yasmin L, Chen X, Stubbs KA, Raston CL. Sci Rep. 2013; 3:2282. [PubMed: 23884385]

11. a) Gandy MN, Raston CL, Stubbs KA. Chem Commun. 2015; 51:11041–11044.b) Gandy MN, Raston CL, Stubbs KA. Org Biomol Chem. 2014; 12:4594–4597. [PubMed: 24887640] c) Vimalanathan K, Chen X, Raston CL. Chem Commun. 2014; 50:11295–11298.d) Chen X, Dobson JF, Raston CL. Chem Commun. 2012; 48:3703–3705.e) Mo J, Eggers PK, Chen X, Ahamed MRH, Becker T, Yong Lim L, Raston CL. Sci Rep. 2015; 5:10414. [PubMed: 26000441]

12. Britton J, Raston CL. RSC Adv. 2015; 5:2276–2280.

13. Yasmin L, Stubbs KA, Raston CL. Tetrahedron Lett. 2014; 55:2246–2248.

14. Bratko I, Mallet-Ladeira S, Saffon N, Teuma E, Gomez M. Dalton T. 2013; 42:1136–1143.

15. Thapaliya ER, Captain B, Raymo FM. J Org Chem. 2014; 79:3973–3981. [PubMed: 24716594]

16. Britton J, Raston CL. RSC Adv. 2014; 4:49850–49854.

17. a) Gutmann B, Cantillo D, Kappe CO. Angew Chem Int Ed. 2015; 54:6688–6728.b) Snead DR, Jamison TF. Angew Chem Int Ed. 2015; 54:983–987.Angew Chem. 2015; 127:997–1001.c) Jas G, Kirschning A. Chem Eur J. 2003; 9:5708–5723. [PubMed: 14673841]

18. Yasmin L, Eggers PK, Skelton BW, Stubbs KA, Raston CL. Green Chem. 2014; 16:3450–3453.

19. Smith NM, Corry B, Swaminathan Iyer K, Norret M, Raston CL. Lab Chip. 2009; 9:2021–2025. [PubMed: 19568670]

20. Yasmin L, Coyle T, Stubbs KA, Raston CL. Chem Commun. 2013; 49:10932–10934.

21. Britton J, Chalker JM, Raston CL. Chem Eur J. 2015; 21:10660–10665. [PubMed: 26095879]

22. Martin AD, Boulos RA, Hubble LJ, Hartlieb KJ, Raston CL. Chem Commun. 2011; 47:7353–7355.

23. Geim AK, Novoselov KS. Nat Mater. 2007; 6:183–191. [PubMed: 17330084]

24. a) Peng W, Chen X, Zhu S, Guo C, Raston CL. Chem Commun. 2014; 50:11764–11767.b) Boulos RA, Zhang F, Tjandra ES, Martin AD, Spagnoli D, Raston CL. Sci Rep. 2014; 4:3616. [PubMed: 24448077]

25. Zhou G-T, Yu JC, Wang X-C, Zhang L-Z. New J Chem. 2004; 28:1027–1031.

26. Vimalanathan K, Shrestha RG, Zhang Z, Zou J, Nakayama T, Raston CL. Angew Chemie Int Ed. 2016; doi: 10.1002/anie.201608673

27. Tong CL, Boulos RA, Yu C, Iyer KS, Raston CL. RSC Adv. 2013; 3:18767–18770.

28. Shibata H, Ogura T, Nishio K, Sakai H, Abe M, Hashimoto K, Matsumoto M. Silicon. 2011; 3:139–143.

29. Wahid MH, Eroglu E, LaVars SM, Newton K, Gibson CT, Stroeher UH, Chen X, Boulos RA, Raston CL, Harmer S-L. RSC Adv. 2015; 5:37424–37430.

30. Britton J, Dyer RP, Majumdar S, Raston CL, Weiss GA. Angew Chem Int Ed. 2017; 56:2296–2301.Angew Chem. 2017; 129:2336–2341.

31. a) Mozhaev VV, Lange R, Kudryashova EV, Balny C. Biotechnol Bioeng. 1996; 52:320–331. [PubMed: 18629899] b) Luong TQ, Erwin N, Neumann M, Schmidt A, Loos C, Schmidt V, Fändrich M, Winter R. Angew Chem Int Ed. 2016; 55:12412–12416.Angew Chem. 128:12600–12604.

32. Britton J, Raston CL, Weiss GA. Chem Commun. 2016; 52:10159–10162.

Biographies

Joshua Britton earned his MSci at the University of Nottingham, UK and undertook his PhD studies at The University of California, Irvine and Flinders University, South Australia with Prof. Gregory A. Weiss and Prof. Colin L. Raston. He is currently a postdoctoral scholar at MIT with Prof. Timothy F. Jamison. His research interests include combining biocatalysis with multi-step continuous flow chemistry for the improved synthesis of bioactive compounds. His awards include the Kipping (*2011*), Syngenta (*2012*) and British Petroleum Award (*2013*) *and* Taihi Hong Memorial award (2015).

Keith Stubbs completed his PhD at the University of Western Australia and undertook postdoctoral studies at Simon Fraser University. He moved back to Australia in 2008 and is currently at the University of Western Australia. His research interests include synthetic organic chemistry, bioorganic chemistry and chemical biology with a focus on carbohydrates. His awards include being a Western Australian Young Tall Poppy for Science and receiving the Rennie Memorial Medal and the Athel Beckwith Lectureship from the RACI.

Gregory Weiss is a Professor of Chemical Biology at U.C. Irvine. He earned a BS from UC Berkeley and PhD from Harvard University. Awarded with a NIH postdoctoral fellowship, he returned the funding to study with Dr. Jim Wells, then at Genentech. His awards include Beckman Young Investigator and AAAS Fellow. His laboratory focuses on the interface between chemistry and biology, including the study of membrane proteins, bioelectronics, and single molecule biophysics. He was awarded an Ig Nobel Prize in Chemistry for leading the team that unboiled a hard-boiled egg.

Colin Raston AO is SA Premier's Professorial Research Fellow in Clean Technology. He completed a PhD with Prof Allan White, and after postdoctoral studies with Prof Michael Lappert at the University of Sussex, was appointed a lecturer at The University of Western Australia then to chairs at Griffith, Monash, Leeds (2001) and UWA (2003), before moving to Flinders University in 2013. Awards from the RACI include the Leighton Memorial Award and his former Presidency. He is an Officer of the Order of Australia and his research interests include nano- and green chemistry as well as microfluidics.
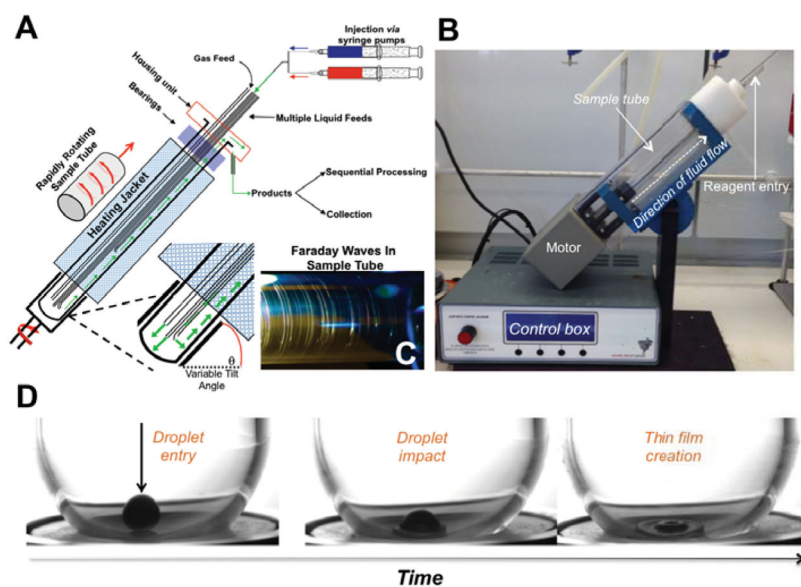
Figure 1.
The vortex fluidic device (VFD). A) A schematic of the VFD highlighting important operational features. Fluids are injected down metal feed jets and into the hemisphere of the sample tube *via* syringe pumps. The injected fluid impacts the sample tube and generates a dynamic thin film that climbs the reactor as more fluid is added. B) A photograph of the VFD. C) The Faraday waves present in the thin film that result from specific rotational speeds. A larger photograph and additional images are available in the Supplementary Information. D) High-speed photographs of reagent entry into a VFD.[6] The first image highlights droplet entry into the reactor, the central image captures its subsequent impact, and the final image shows the creation of the thin film. For further information on the fluid dynamic considerations of the VFD, see previous publications.[6–7]
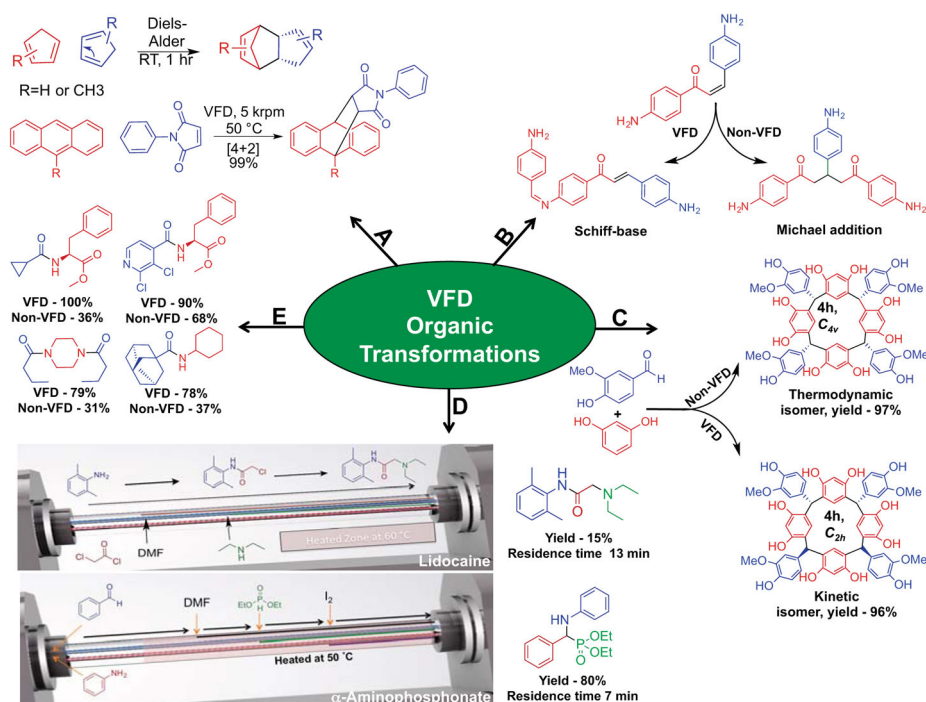
Figure 2.
Examples of VFD-mediated synthetic transformations. A) The [4+2] Diels-Alder reaction of two cyclopentadiene molecules as well as the [4+2] Diels-Alder between anthracene and N-phenylmaleimide; no conversion results from identical conditions in the non-VFD control. [10] [13] B) Processing under high mass and heat transfer in the VFD favors the Michael-addition product; by contrast, in a non-VFD control, the Schiff base product is favored.[19] C) The stereoselective synthesis of resorcin[4]arenes and pyrogallo[4]arenes in the VFD, with the VFD favoring the kinetic isomer over the thermodynamic isomer.[20] D) Assembly line synthesis of lidocaine through sequential, spatially segregated transformations and the assembly line-inspired synthesis of an α-aminophosphonate utilizing *in situ* solvent exchange to drive a multi-step transformation. [21] [8] E) The synthesis of amides through the coupling of acyl chlorides with amines. Products were isolated through silica column chromatography with >95% purity observed by ^{1}H NMR analysis.
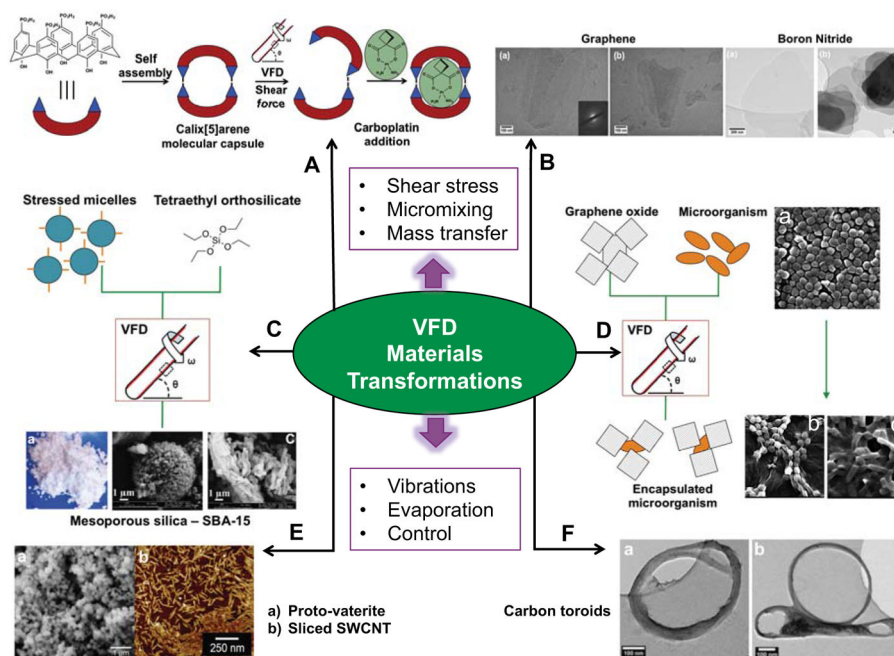
Figure 3.
VFD-mediated materials transformations. A) *p*-Phosphonate-calix[5]arene molecular capsules undergo H-bonding disruption (disassembly) under the shear stress for loading carboplatin post-VFD processing.[22] B) TEM images of exfoliated graphite and hexagonal boron nitride.[11d] C) Continuous flow processing of SBA-15 mesoporous silica where shear stressed micelles are mixed with triethyl orthosilicate (TEOS) and the resulting material filtered and calcined, as with SEM images B and C.[26–27] D) VFD-mediated encapsulation of *staphylococcus aureus* and *rhodococcus opacus* graphene oxide sheets, SEM A - *Staphylococcus aureus* before processing in the VFD, SEM B - *Staphylococcus aureus* encapsulated in graphene oxide and SEM C - *Rhodococcus opacus* encapsulated in graphene oxide.[29] E) Controlling the rotational speed of the sample tube allows access to metastable forms of calcium carbonate such as proto-vaterite (SEM A), and sliced SWCNT (SEM B).[9b, 24] F) Toroids of self assembled SWCNT in a 1:1 water: toluene solvent mixture, where the high shear stress bends the SWCNT around the hydrophobic-hydrophilic interface.[11c]
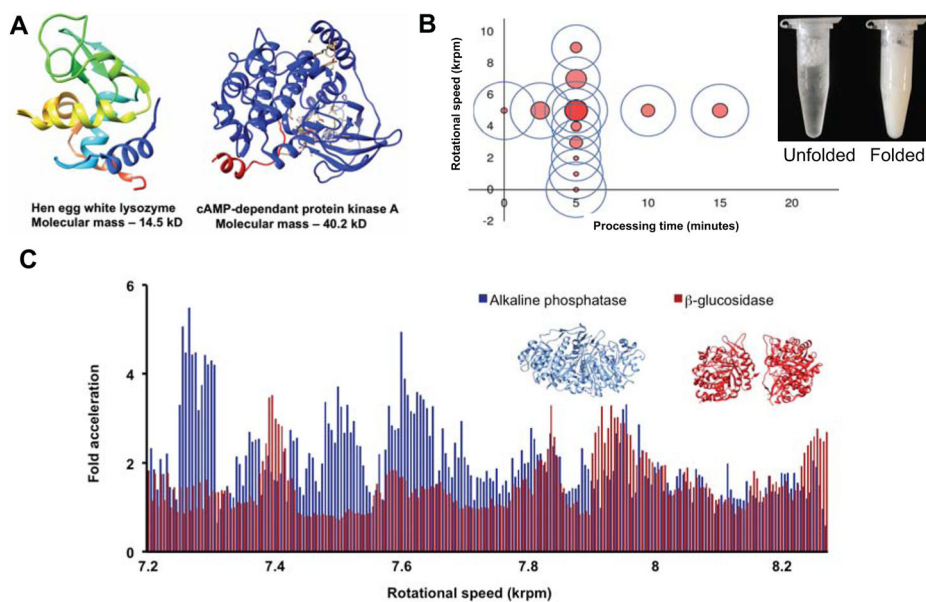
Figure 4.
An overview of VFD-mediated biochemical transformations. A) Hen egg white lysozyme (HEWL) as a smaller protein with a molecular mass of 14.5 kDa and cAMP-dependant protein kinase A (PKA) as a larger protein with a molecular mass of 40.2 kDa. Both proteins were folded *via* VFD-mediated processing with a 100-fold decrease in refolding time.[7a] B) The dependency on the rotational speed of the sample tube on the capability of the VFD to refold HEWL, with rotational speed of 5.00 krpm for a 10 mm external diameter tube being effective. C) The acceleration landscapes for alkaline phosphatase and β-glucosidase compared to the non-VFD control. The specific rotational speeds needed to accelerate each enzyme hints towards a tertiary structure dependency on the correct rotational speed. For error calculations and statistical analysis of the data, see the original publication.[9a] D) An array of 28 stripes of mCherry and GFP protein on the inner surface of the VFD sample tube. Stripes are created through rapid bioconjugation of proteins fused to His_n-tags through immobilized metal affinity chromatography (IMAC) resin bound to the inner surface of the sample tube.[29]